JOURNAL OF NANO- AND ELECTRONIC PHYSICS
Vol. **4** No 3, 03016(6pp) (2012)

ЖУРНАЛ НАНО- ТА ЕЛЕКТРОННОЇ ФІЗИКИ
Том **4** № 3, 03016(6cc) (2012)

Influence of Substrate on Magnetoresistive and Magneto-Optical Properties of Co/Fe Film System

O.V. Fedchenko[1,*], A.I. Saltykova[2], S.I. Protsenko[1]

[1] *Sumy State University, 2, Rimsky-Korsakov Str., 40007 Sumy, Ukraine*
[2] *Sumy State Pedagogical University of A.S. Makarenko, 87, Romens'ka Str., 40002 Sumy, Ukraine*

(Received 25 September 2012; in final form 14 October 2012; published online 29 October 2012)

The influence of substrate material on the magnetoresistive, magneto-optical properties and diffusion processes in Co(30 nm)/Fe(30 nm)/S was investigated. The samples were built on amorphous SiO_2/Si substrate and MgO(100) crystal and then were annealed up to 300, 500 and 800 °C. Control of the crystal structure and sample elemental composition was held by the low-energy electron diffraction (LEED) and energy dispersive X-ray analysis (EDX). After that magnetoresistive properties (MR) and magneto-optical Kerr effect (MOKE) were investigated and diffusion profiles were built with the help of secondary ion mass spectroscopy (SIMS).

It was stated that during oriented growth of film system on MgO(100) crystal the considerable magnetic anisotropy is observed. It appears in increase of coercive force (B_C) in two times and significant variation of magnetoresistance at different turn angles. AFM investigations showed that surface roughness of Au(2 nm)/Co(30 nm)/Fe(30 nm)/MgO film system is four times lower than of the sample on amorphous substrate (non-annealed). Besides the diffusion processes in systems that were built on MgO monocrystal proceed less intensive than in the case of SiO_2/Si.

Keywords: Magnetoresistive properties, Kerr effect, Magnetic anisotropy, Diffusion profile, Coercive force.

PACS numbers: 75.70.Cn, 81.15.Np

1. INTRODUCTION

The structures based on nanosized film systems are widely used as an element base of microelectronics. They have found an application in sensors (of pressure, position, current, magnetic field), biosensors, hard disc read heads, spin transistors, etc. Modern recording devices widely use soft magnetic materials with specified anisotropy and high saturation field [1]. From this point of view, Fe/Co-based multilayer structures have obtained a wide spread, since their magnetic characteristics can be changed by annealing or ion beam treatment [2]. Moreover, material and structural state of a substrate influence the sample properties that determines the film growth mechanisms. Therefore, the aim of the present paper is to establish the correlation between magneto-optical and magnetoresistive properties and diffusion processes in Fe/Co/S system and annealing temperature and substrate material.

2. EXPERIMENTAL TECHNIQUE

Film system based on Fe and Co was deposited in vacuum 7×10^{-8} Pa. MgO(100) crystal and SiO_2/Si were used as the substrates in order to realize the directional film growth and growth on amorphous substrate, respectively. Magnesium oxide crystal was chosen due to the fact that it allows to realize epitaxial growth of Fe, since for Fe(100)||MgO(100) orientation the difference between the lattice parameters is not more than 3,8%: a = 2,87 Å for the bcc-Fe and a = 2,98 Å for the fcc-MgO (between Mg or O atoms, since lattice is of the NaCl type) [3]. In this case, zero-defect epitaxy with elastic mismatch compensation takes place [4]. Moreover, Fe/Co system based on MgO at certain deposition conditions can have unique magnetic properties and be used for magnetic recording [5, 6], be the base for formation of the electron spin-filter [7], etc.

For loading into vacuum chamber, substrates were cleaned by ultrasound in acetone and isopropanol, and then they were annealed in vacuum 10^{-8} Pa at 570 °C during 60 min. Deposition rates of Co and Fe atoms were equal to ω = 0,15 and 0,12 nm/min, respectively, that provided epitaxial growth. Fe films were deposited on heated up to 180 °C substrate; at this temperature islands have the minimum roughness [8]. After sputtering of Fe layer, samples were annealed at 450 °C during 20 min. In this case, the bcc-Fe lattice, but not the tetragonal lattice [3], is formed even in the thinnest layers (thickness to 1 nm).

Quality control of MgO substrate cleaning and Fe epitaxial growth were carried out by using the low-energy electron diffraction (LEED) (Fig. 1).

Presence of reflexes in Fig. 1 indicates the atomically clean surface [9]. Moreover, Fig. 1a confirms the fact that MgO has the NaCl type lattice, and Fig. 1b corresponds to the bcc-Fe. If compare ratios of Mg/Fe lattice parameters for one energy value (for example, 131 eV), then deviation of our experimental data of the LEED-investigations from the calculated ones is about ≅ 7% (1,47 un. – calculated [3] and 1,57 un – experimental data). This difference can be explained by different operating modes of the Wehnelt cylinder and lens of the LEED-system when obtaining images from MgO and Fe surface [9]. Moreover, one should take into account that LEED-images for Fe films were obtained at the thickness of d ≅ 30 nm, and misfit dislocations appear in this case and Fe layer is not pseudomorphous any more [4].

Thickness of the samples was controlled by quartz resonator. After preparation of the film systems, they were deposited by Au layer with d ≅ 2 nm to prevent air

* fedchenko.lena@gmail.com

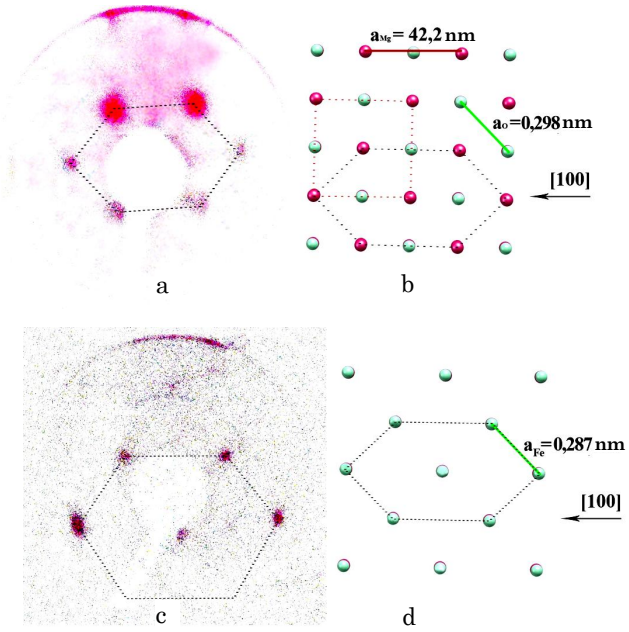

Fig. 1 – LEED-image from the MgO(100) substrate at the energy of 165 eV (a) and schematic representation of the MgO crystal structure (lattice of the NaCl type) (b) in the plane containing direction [100]; LEED-image from Fe(30 nm)/MgO(100) film at the energy of 106 eV (c) and image of the bcc-Fe crystal structure in the plane containing direction [100] (d)

oxidation. Annealing of the samples in vacuum 10^{-8} Pa at 300, 500, and 800 °C took place then. Samples were held during 30 min at each temperature.

Presence of impurities in the obtained samples was checked on by the energy-dispersion X-ray spectroscopy (EDX) using add-on WINEDS High Performance X-ray Microanalysis at PEM JSM-6400. In Fig. 2 we present the obtained spectra for Au(2)/Co(30)/Fe(30)/MgO and Au(2)/Co(30)/ Fe(30)/SiO_2/Si systems.

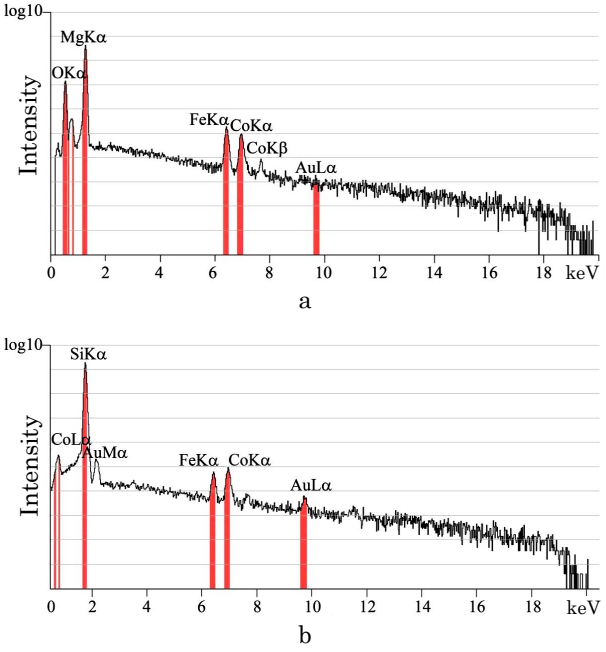

Fig. 2 – The EDX spectra for Au(2)/Co(30)/Fe(30)/MgO (a) and Au(2)/Co(30)/Fe(30)/SiO_2/Si (b) systems

As seen from Fig. 2, spectra do not have additional peaks except Fe, Co, Au, Si, Mg, and O that implies the purity of the obtained samples.

Control of the surface structure was performed by the atomic-force microscope (AFM) of SIScan Company, which allowed to determine the surface roughness, obtain distributions of inhomogeneities by sizes, and 3D-images of a part of the sample interface.

Then magnetic characteristics of unannealed systems and annealed ones to the temperatures of 300, 500, and 800 °C were studied. The MOKE investigations were carried out at different turn angles of the samples in its plane, MR was fixed at the turn relative to the axis which is parallel to the sample surface (in the range of 0-90°). In both cases two measurement geometries were used: longitudinal and perpendicular ones for MOKE, and longitudinal and transverse geometries for MR. The necessity of such investigations is conditioned by the problems of discovery of magnetic anisotropy. Moreover, visualization of remagnetization of system domains by using MOKE-microscopy was done.

The SIMS investigations were carried out to define the substrate influence on the diffusion processes; this allowed to obtain diffusion profiles. The etching rate was sufficiently low (0,5 nm/min) that maximally decreased the influence of the ion-stimulated diffusion (ISD).

3. ANALYSIS OF THE OBTAINED RESULTS

In Fig. 3 we represent the AFM-images in the mode of surface topology of the samples grown on MgO(100) monocrystal and SiO_2/Si amorphous substrate.

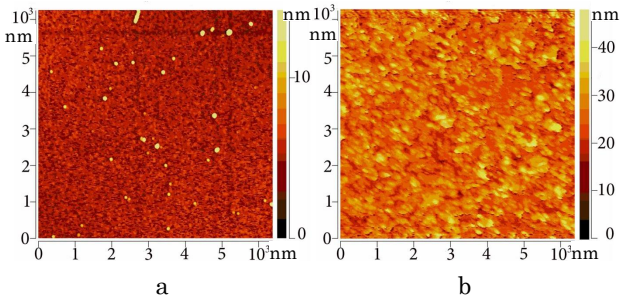

Fig. 3 – AFM-images in the topology mode for the following systems without annealing: Au(2)/Co(30)/Fe(30)/MgO (a) and Au(2)/Co(30)/Fe(30)/SiO_2/Si (b)

As seen from Fig. 3, roughness of the system, which is directionally grown, is approximately four times less. This is confirmed by the calculations of the root-mean-square (rms) deviations of irregularity σ. $\sigma \cong 1{,}4$ nm is the rms for Au(2)/Co(30)/Fe(30)/MgO and 4,6 nm – for Au(2)/Co(30)/Fe(30)/SiO_2/Si. The average size of islands is equal to 140 nm for substrate-monocrystal (Fig. 1a) and ≈ 210 nm – for amorphous substrate (Fig. 1b).

During annealing of the Au(2)/Co(30)/Fe(30)/SiO_2/Si system up to 300 °C, the surface roughness considerably decreased ($\sigma \cong 1{,}2$ nm) that can be explained by the surface diffusion of atoms. At further increase in the temperature up to 500 °C and 800 °C, the average size of islands increased (Fig. 4). By the calculations based on the represented profiles it was 70 nm at 300 °C and 200 nm at 800 °C.

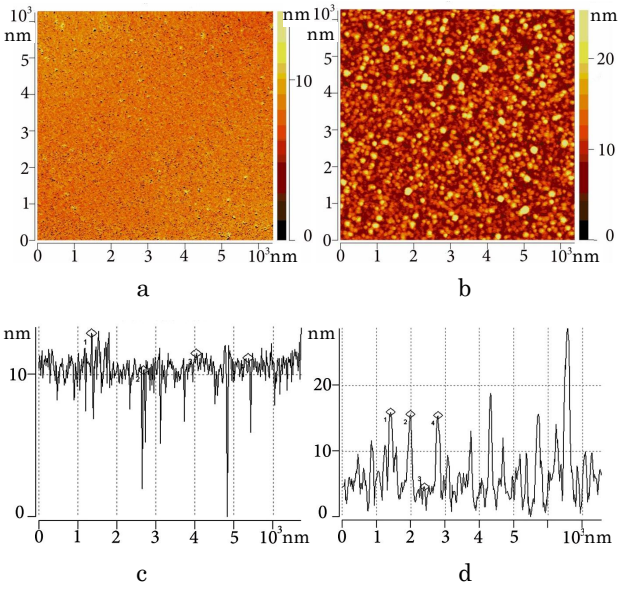

Fig. 4 – The AFM-images and surface profiles of the system Au(2)/Co(30)/Fe(30)/SiO_2/Si at annealing up to 300 °C (a, c) and 800 °C (b, d)

Investigations of the magnetoresistance have shown that system epitaxially grown on MgO(100) substrate displays anisotropy at different turn angles of the samples with respect to the magnetic field. This occurs during both the transition from the perpendicular geometry to the longitudinal one and to the transverse geometry (Fig. 5a,b). Samples obtained on amorphous substrate have constant dependences (Fig. c,d).

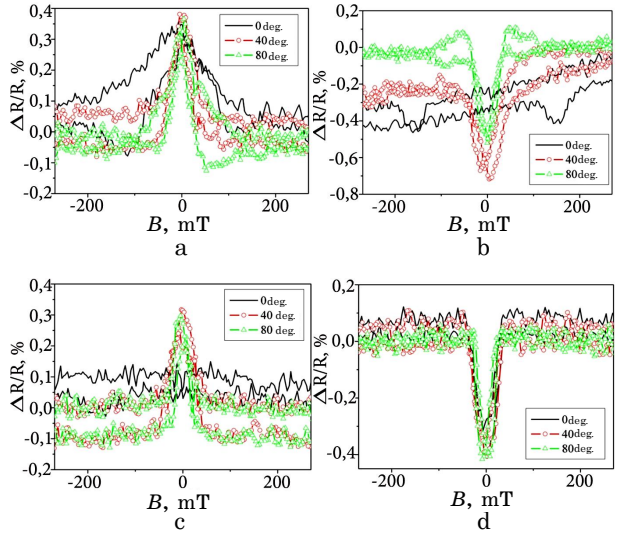

Fig. 5 – Dependences of the MR on the turn angle of the sample for the following systems: Au(2)/Co(30)/Fe(30)/MgO (a, b) and Au(2)/Co(30)/Fe(30)/SiO_2/Si (c, d) at the transition from the perpendicular geometry (a, c) to the longitudinal one (b, d)

After annealing of the samples up to 300 °C, the magnetoresistance of Au(2)/Co(30)/Fe(30)/MgO system sharply decreases, especially this is evident at the transition from the perpendicular to the longitudinal geometry (Fig. 6a,b). In Au(2)/Co(30)/Fe(30)/SiO_2/Si system, inversely, magnetoresistive properties remain and MR is changed insignificantly (Fig. c,d).

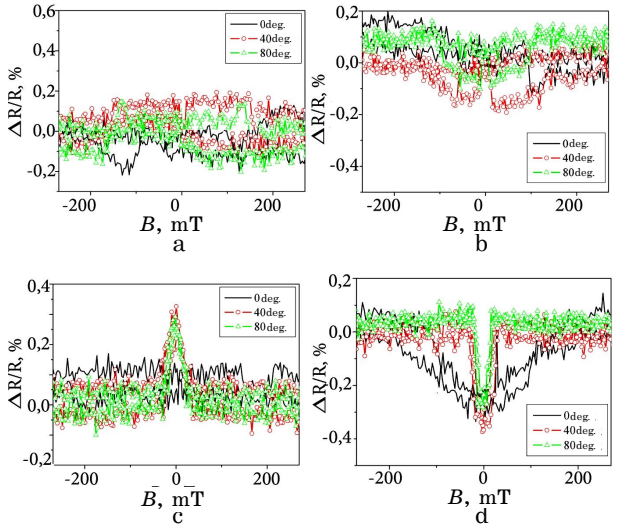

Fig. 6 – Dependences of the MR on the turn angle of the sample for the following systems: Au(2)/Co(30)/Fe(30)/MgO (a, b) and Au(2)/Co(30)/Fe(30)/SiO_2/Si (c, d) annealed up to 300 °C at the transition from the perpendicular to the transverse (a, c) and from the perpendicular to the longitudinal geometry (b, d)

But at annealing up to 500 °C, magnetoresistance disappears completely in Au(2)/Co(30)/Fe(30)/SiO_2/Si system at two measurement geometries, too.

In Fig. 7 we represent the magneto-optical dependences at the longitudinal measurement geometry for Au(2)/Co(30)/Fe(30)/MgO and Au(2)/Co(30)/Fe(30)/SiO_2/Si systems (Fig. 7a,b). Manifestation of the magnetic anisotropy in the case of the directed growth of the sample on MgO(100) monocrystal is clearly seen in this figure. In Fig. 7c,d in polar coordinates we show the dependences of the coercive force (B_c) on the turn angle of the sample relative to the axis perpendicular to the sample surface. It is seen that for a system on MgO substrate, the external view of this dependence is considerably changed after annealing up to 300 °C that indicates the presence of the diffusion processes. Moreover, just after annealing to this temperature, magnetoresistance of Au(2)/Co(30)/Fe(30)/MgO structure significantly decreases (Fig. 6a,b) that can also imply the formation of an intermediate layer due to diffusion. As it is known, the sample with Fe(100)||MgO(100) orientation possesses anisotropy which is appeared during the sample turn by 45° that is confirmed by Fig. 7c (two-fold increase in the coercive force is observed along these directions).

Co films and Fe/Co systems have uniaxial anisotropy even if they are grown on amorphous substrates [10, 1, 2]. Therefore, a sample on SiO_2/Si also exhibits magnetic anisotropy.

Dependences of the coercive force on the turn angle for Au(2)/Co(30)/Fe(30)/SiO_2/Si system are not changed significantly in shape at annealing up to 300 °C. This can imply a small intensity of phase transformations [11]. Moreover, constant magnetoresistive properties at the annealing temperature of 300 °C in comparison with initial ones confirm the above mentioned statement. Probably, in Au(2)/Co(30)/Fe(30)/SiO_2/Si system diffusion processes are more intensive during condensation. Therefore, the value of magnetoresistance for this sample is considerably less than for the system on monocrystal substrate (Fig. 5): MR ≈ 0,3% and 0,4% in the

case of SiO_2/Si substrate and MR ≈ 0,4% and 0,7% for MgO substrate, respectively, for the transition from the perpendicular to the transverse and to the longitudinal geometry. Further annealing up to 300 °C does not lead to the intense diffusion processes but promotes healing of defects and decrease in the layer roughness that, in turn, makes easier the propagation of domain walls and leads to the decrease in the coercive force [12]. In this case, the crystallite size is not changed significantly [11] that is confirmed by the AFM-image (Fig. 4a).

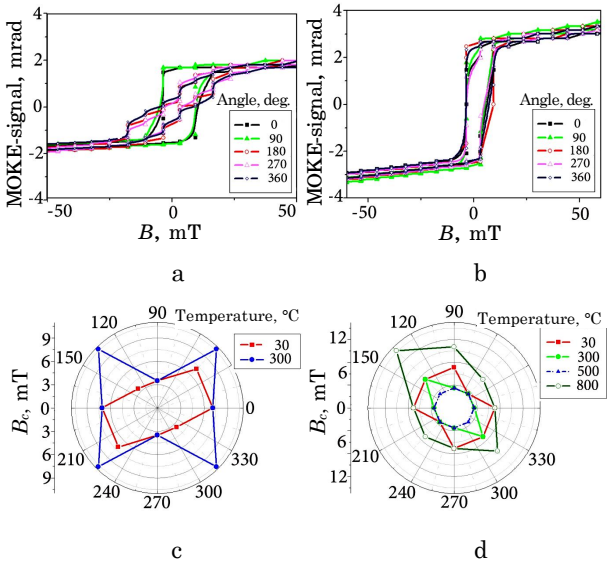

Fig. 7 – Magneto-optical dependences at the longitudinal measurement geometry for the systems Au(2)/Co(30)/Fe(30)/MgO (a) and Au(2)/Co(30)/Fe(30)/SiO_2/Si after annealing up to 500 °C (b) at different turn angles of the sample; dependences of the coercive force on the turn angle in polar coordinates at different annealing temperatures for Au(2)/Co(30)/Fe(30)/MgO (c) and Au(2)/Co(30)/Fe(30)/SiO_2/Si (d)

Further annealing up to 500 °C changes the behavior of the dependence of the coercive force on the turn angle (anisotropy disappears) (Fig. 7d) and leads to the decrease in the value of B_c. Most likely, these phenomena are caused by the formation of solid solution with introduction of Co nanogranules in the sample interior. Moreover, exactly in this moment MR completely disappears in both geometries (Fig. 7).

During annealing up to 800 °C, coercive force rapidly increases. This can be explained by the increase in the average size of Co granules. The AFM-image (Fig. 4b) confirms this assumption. Thus, during annealing of Au(2)/Co(30)/Fe(30)/SiO_2/Si system, coercive force firstly decreases and after 500 °C it rapidly increases. The authors of the work [11] point that based on the external view of the MR and MOKE dependences we can judge the presence of one or another structural state of the system. Typical view of the dependences of the Kerr turn on the magnetic field induction for the system Au(2)/Co(30)/Fe(30)/SiO_2/Si without and after annealing (up to 800 °C) indicates the presence of multilayer structure and granular solid solution, respectively.

Dependences of the coercive force on the turn angles of the samples were confirmed using the MOKE-microscopy which allows to visualize the processes of domain remagnetization [13] (Fig. 8). For Au(2)/Co(30)/Fe(30)/SiO_2/Si system, total remagnetization at the sample rotation by 45° occurs at 7 mT (Fig. 8a), and at the sample rotation by 90° – at 3,4 mT (Fig. 8b). Obtained results imply almost a two-fold difference in B_c at these turn angles (see Fig. 7c).

As for Au(2)/Co(30)/Fe(30)/MgO system after annealing up to 800 °C, the results of the Kerr microscopy have shown the total remagnetization at 7,5 mT that completely corresponds to the dependence represented in Fig. 7d.

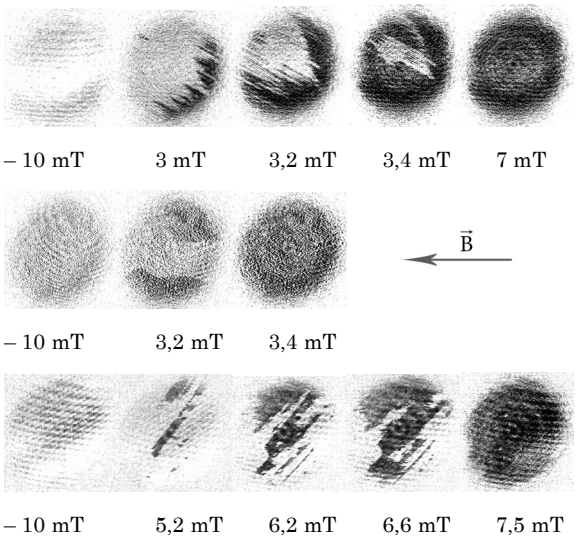

Fig. 8 – Images of the MOKE-microscopy in the longitudinal geometry for Au(2)/Co(30)/Fe(30)/MgO system at the sample rotation by 45° (a), 90° (b) and for Au(2)/Co(30)/Fe(30)/SiO_2/Si system after annealing up to 800 °C at the rotation by 45° (c)

Diffusion profiles (Fig. 9) which allowed to estimate the effective coefficients of atomic diffusion in film systems were obtained based on the investigations by the SIMS method. Dependences represented in Fig. 9a-e indicate different intensity of the diffusion processes for systems on MgO(100) and SiO_2/Si substrates and influence of the Kirkendall effect on the interface shift [14] in both cases. Estimation of the influence of the condensation-stimulated (CSD) and the ion-stimulated (ISD) diffusion on the diffusion profiles was performed using the following correlation:

$$D_k = l_k^2/\tau_k, \qquad (1)$$

where l_k is the length of the diffusion path of atoms; τ_k is the time of condensation [15, 16].

Calculation of the effective coefficients of thermal diffusion (TD) was realized as follows:

$$D_{m\partial} = \Delta l/\tau_m = (l_m - l_k)^2/\tau_m, \qquad (2)$$

where l_m is the length of the diffusion path of atoms in the case of TD; τ_m is the annealing time of the system.

It is seen from Fig. 9a,b that in both systems during condensation diffusion of atoms of the upper layer (Co) to the lower one is more intensive than in the opposite direction. Moreover, intensity of the diffusion processes (in both directions) for the system grown directionally on MgO(100) substrate is slightly lower in comparison with Au(2)/Co(30)/Fe(30)/SiO_2/Si system (Table 1). This

Table 1 – Effective coefficients of diffusion of atoms in Au(2)/Co(30)/Fe(30)/MgO and Au(2)/Co(30)/Fe(30)/SiO_2/Si film systems

Substrate	Diffusion vapor	CSD, CSD + ISD		TD					
				T_{ann} = 300 °C		T_{ann} = 500 °C		T_{ann} = 800 °C	
		l, nm	$D_c \cdot 10^{19}$, m²/s	l, nm	$D_{td} \cdot 10^{19}$, ($D_t \cdot 10^{19}$) m²/s	l, nm	$D_t \cdot 10^{19}$, m²/s	l, nm	$D_t \cdot 10^{19}$, m²/s
MgO(100)	Fe → Co	24	21,3	17	0,27	–	–	–	–
	Co → Fe	27	33,8	30	0,05	–	–	–	–
SiO_2/Si	Fe → Co	27	27,0	24	0,05	30	5	30	5
	Co → Fe	30	41,7	30	5,00	30	5	30	5

explains larger MR values in Au(2)/Co(30)/Fe(30)/MgO system in comparison with the sample on amorphous substrate (see Fig. 5). After annealing up to 300 °C, the effective diffusion coefficient decreases almost by two orders of magnitude that indicates the beginning of the diffusion in the grain interior. At the temperature of T_{ann} = 500 °C in Au(2)/Co(30)/Fe(30)/SiO_2/Si system one can observe a complete mixing of atoms that leads to the MR disappearance in both geometries.

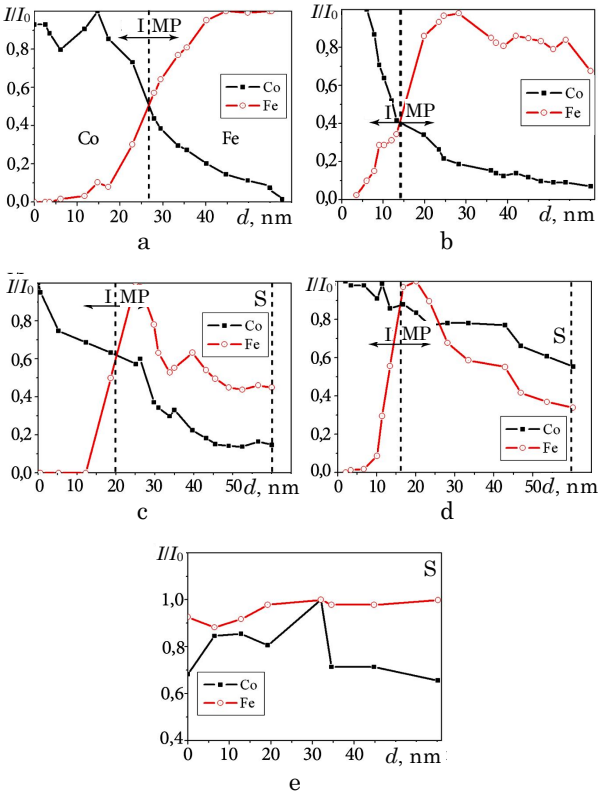

Fig. 9 – Diffusion profiles for Au(2)/Co(30)/Fe(30)/MgO (a, c) and Au(2)/Co(30)/Fe(30)/SiO_2/Si (b, d, e) film systems in unannealed (a, b) and annealed up to 300 °C (c, d) and 800 °C (e); I – interface, MP – Matano plane, S – substrate

Thus, substrate material significantly influences the diffusion processes in the system and, correspondingly, its magnetic properties. However, obtained values of the effective diffusion coefficients can be slightly overrated because of the presence of the ISD effect.

4. CONCLUSIONS

It is established in the work that substrate material, its structural state significantly influence the magnetoresistive, magneto-optical properties and the diffusion processes in film systems. Namely, at the directional growth on MgO(100) monocrystal Au(2)/Co(30)/Fe(30)/MgO system displays considerable anisotropy of the magnetoresistance and coercive force (there is a 2-fold increase in B_c at the sample rotation by 45°). In both measurement geometries MR is slightly higher than for Au(2)/Co(30)/Fe(30)/SiO_2/Si system that is explained by the lower intensity of the diffusion processes during condensation. At annealing up to 300 °C MR of the directionally grown sample almost disappears. For the system on amorphous substrate such phenomenon is observed during annealing up to 500 °C.

At different annealing temperatures of Au(2)/Co(30)/Fe(30)/SiO_2/Si system, coercive force at first decreases, and after 500 °C it starts to rapidly increase. This can be explained by the formation of solid solution with Co nanogranules whose size increases at annealing up to 800 °C that leads to the growth of B_c.

Moreover, in unannealed state system which was condensed on amorphous substrate has four times more roughness than at condensation on monocrystal.

AKNOWLEDGEMENTS

The work has been performed under the financial support of the Ministry of Education and Science, Youth and Sport of Ukraine (state registration number 0112U001381).

REFERENCES

1. R. Gupta, A. Khandelwal, R. Ansari, K.G.M. Nair, *Surf. Coat. Tech.* **203**, 2717 (2009).
2. M. Rateo, M. Carbucicchio, M. Ghidini, M. Solzi, *J. Magn. Magn. Mater.* **272**, 1240 (2004).
3. A. di Bona, C. Giovanardi, S. Valeri, *Surf. Sci.* **498** 193 (2002).
4. I.Yu. Protsenko, N.I. Shumakova, *Tekhnologiya oderzhannya i zastosuvannya plivkovyh materialiv* (Sumy: vyd-vo SumDU: 2007).
5. *Y.* Park, S. Adenwalla, G.P. Felcher, S.D. Bader, *Phys. Rev. B* **52**, 12779 (1995).
6. Y.Y. Huang, C. Liu, G.P. Felcher, *Phys. Rev. B* **47**, 183 (1993).
7. R. Bertacco, F. Ciccacci, *J. Magn. Magn. Mater.* **196-197**, 134 (1999).
8. J.F. Lawler, R. Schad, S. Jordan, H. van Kempen, *J. Magn. Magn. Mater.* **165**, 224 (1997).
9. G. Ertl, J. Kueppers, *Low Energy Electrons and Surface*

Chemistry, 374 (Weinheim: Betz-druck gmbh: 1985).
10. .F.J.B. Wedding, M. Li, G.-C. Wang, *J. Magn. Magn. Mater.* **204**, 79 (1999).
11. F. Spizzo, E. Angeli, D. Bisero, *J. Magn. Magn. Mater.* **242**, 473 (2002).
12. X. Lin, G. Ji, T. Gao, X. Chang, Y. Liu, H. Zhang, Y. Du, *Solid State Commun.* **151**, 1708 (2011).
13. J.M. Teixeira, R.F.A. Silva, J. Ventura, A.M. Pereira, *Mater. Sci. Eng. B* 1**26**, 180 (2006).
14. A. Paul, M.J.H. van Dal, A.A. Kodentsov, F.J.J. van Loo, *Acta Mater.* **52**, 623 (2004).
15. O. Fedchenko, S. Protsenko, P. Zukowski, M. Marszalek, *Vacuum* **86**, 1934 (2012).
16. M.G. Demydenko, S.I. Protsenko, K.V. Tyschenko, O.V. Fedchenko, *J. Nano- Electron. Phys.* **4** No2, 38 (2012).